Theoret. Appl. Mech., Vol.36, No.3, pp. 239-260, Belgrade 2009

Radiation and mass transfer effects on unsteady MHD free convection flow of an incompressible viscous fluid past a moving vertical cylinder

M.Gnaneswara Reddy * **N.Bhaskar Reddy** †

Abstract

The interaction of free convection with thermal radiation of a viscous incompressible unsteady MHD flow past a moving vertical cylinder with heat and mass transfer is analyzed. The fluid is a gray, absorbing-emitting but non-scattering medium and the Rosseland approximation is used to describe the radiative heat flux in the energy equation. The governing equations are solved using an implicit finite-difference scheme of Crank-Nicolson type. Numerical results for the transient velocity, the temperature, the concentration, the local as well as average skin-friction, the rate of heat and mass transfer for various parameters such as thermal Grashof number, mass Grashof number, magnetic parameter, radiation parameter and Schmidt number are shown graphically. It is observed that, when the radiation parameter increases the velocity and temperature decrease in the boundary layer. Also, it is found that as increase in the magnetic field leads to decrease in the velocity field and rise in the thermal boundary thickness.

Keywords: Heat transfer, Radiation, Finite-difference Scheme, Vertical cylinder

*Department of Mathematics, Sri Venkateswara University, Tirupati, India - 517 502, e-mail: mgrsvu@gmail.com

†Department of Mathematics, Sri Venkateswara University, Tirupati, India - 517 502

1 Introduction

The study of unsteady boundary layer flow over a moving vertical cylinder has important geophysical and engineering applications. For example, as a result of volcanic activities or tectonic movements, magmatic intrusion may occur at shallow depths in the earth's crust. The intrusive magma may take the form of a cylindrical shape. An experimental and analytical study is reported by Evas et al. [1] for transient natural convection in a vertical cylinder. Velusamy and Grag [2], given a numerical solution for the transient natural convection over a heat generating vertical cylinder.

The study of flow problems, which involve the interaction of several phenomena, has a wide range of applications in the field of science and technology. One such study is related to the effects of MHD free convection flow, which plays an important role in geophysics, astrophysics and petroleum industries. Michiyoshi et al. [3] considered natural convection heat transfer from a horizontal cylinder to mercury under a magnetic field. Magnetic field effect on a moving vertical cylinder with constant heat flux was given by Ganesan and Loganathan [4].

Free convection flow involving coupled heat and mass transfer occures frequently in nature. It occures not only due to temperature differences, but also due to concentration differences or a combination of these two, for example, in atmospheric flows there exist differences in the H_20 concentration. A few representative fields of interest in which combined heat and mass transfer plays an important role are designing of chemical processing equipment, formation and dispersion of fog, distribution of temperature and moisture over agricultural fields and groves of fruit trees, crop damage due to freezing, and environmental pollution. The effects of heat and mass transfer on natural convection flow over a vertical cylinder was studied by Chen and Yuh [5]. Combined heat and mass transfer effects on moving vertical cylinder for steady and unsteady flows were analyzed by Takhar et al. [6] and Ganesan and Loganathan [7] respectively. A numerical solution for the transient natural convection flow over a vertical cylinder under the combined buoyancy effect of heat and mass transfer was given by Ganesan and Rani [8], by employing an implicit finite-difference scheme. Shanker and Kishan [9] presented the effect of mass transfer on the MHD flow past an impulsively started infinite vertical plate. Ganesan and Rani [10] studied the MHD unsteady free convection flow past a vertical cylinder with

heat and mass transfer.

In the context of space technology and in processes involving high temperatures, the effects of radiation are of vital importance. Studies of free convection flow along a vertical cylinder or horizontal cylinder are important in the field of geothermal power generation and drilling operations where the free stream and buoyancy induced fluid velocities are of roughly the same order of magnitude. Many researchers such as Arpaci [11], Cess [12], Cheng and Ozisik [13], Raptis [14], Hossain and Takhar [15, 16] have investigated the interaction of thermal radiation and free convection for different geometries, by considering the flow to be steady. The unsteady flow past a moving vertical plate in the presence of free convection and radiation were studied by Das et al. [17]. Radiation and mass transfer effects on two-dimensional flow past an impulsively started isothermal vertical plate were studied by Ramachandra Prasad et al. [18]. The combined radiation and free convection flow over a vertical cylinder was studied by Yih [19]. Radiation and mass transfer effects on flow of an incompressible viscous fluid past a moving vertical cylinder was studied by Ganesan and Loganathan [20].

However, the interaction of radiation with mass transfer in an electrically conducting fluid past a moving vertical cylinder has received a little attention. Hence, the object of this paper is to study the radiation and mass transfer effects on hydromagnetic free convection flow of a viscous incompressible optically thick fluid past a moving vertical cylinder. The governing boundary layer equations along with the initial and boundary conditions are first cast into a dimensionless form and the resulting system of equations are then solved by an implicit finite-difference scheme of Crank-Nicolson type. The behaviour of the velocity, temperature, concentration, skin-friction, Nusselt number and Sherwood number has been discussed for variations in the governing thermophysical and hydrodynamical parameters.

2 Mathematical Analysis

A two-dimensional unsteady free convection flow of a viscous incompressible electrically conducting and radiating optically thick fluid past an impulsively started semi-infinite vertical cylinder of radius r_0 is considered.

Here the x-axis is taken along the axis of cylinder in the vertical direction and the radial coordinate r is taken normal to the cylinder. Initially, the fluid and the cylinder are at the same temperature T'_∞ and the concentration C'_∞. At time $t' > 0$, the cylinder starts moving in the vertical direction with velocity u_0 and the surface of the cylinder is raised to a uniform temperature T'_w and concentration C'_w and are maintained constantly thereafter. A uniform magnetic field is applied in the direction perpendicular to the cylinder. The fluid is assumed to be slightly conducting, and hence the magnetic Reynolds number is much less than unity and the induced magnetic field is negligible in comparison with the applied magnetic field. It is further assumed that there is no applied voltage, so that electric field is absent. It is also assumed that the radiative heat flux in the x-direction is negligible as compared to that in the radial direction. The viscous dissipation is also assumed to be negligible in the energy equation due to slow motion of the cylinder. Also, it is assumed that there is no chemical reaction between the diffusing species and the fluid. It is also assumed that all the fluid properties are constant except that of the influence of the density variation with temperature and concentration in the body force term (Boussinesq's approximation). The foreign mass present in the flow is assumed to be at low level and hence Soret and Dufour effects are negligible. Then, the flow under considereation is governed by the following system of equations

Continuity equation

$$\frac{\partial\,(ru)}{\partial\,x} + \frac{\partial(rv)}{\partial\,r} = 0 \tag{1}$$

Momentum equation

$$\frac{\partial\,u}{\partial\,t'} + u\,\frac{\partial\,u}{\partial\,x} + v\,\frac{\partial\,u}{\partial\,r} = g\,\beta\,(T' - T'_\infty) + g\,\beta^*(C' - C'_\infty) + \frac{\nu}{r}\frac{\partial}{\partial r}\left(r\frac{\partial u}{\partial r}\right) - \frac{\sigma\,B_0^2}{\rho}u \tag{2}$$

Energy equation

$$\frac{\partial\,T'}{\partial\,t'} + u\,\frac{\partial\,T'}{\partial\,x} + v\,\frac{\partial\,T'}{\partial\,r} = \frac{\alpha}{r}\frac{\partial}{\partial r}\left(r\frac{\partial T'}{\partial r}\right) - \frac{1}{\rho\,c_p}\frac{1}{r}\frac{\partial}{\partial r}\,(rq_r) \tag{3}$$

Mass diffusion equation

$$\frac{\partial\,C'}{\partial\,t'} + u\,\frac{\partial\,C'}{\partial\,x} + v\,\frac{\partial\,C'}{\partial\,r} = \frac{D}{r}\frac{\partial}{\partial r}\left(r\frac{\partial C'}{\partial r}\right) \tag{4}$$

The initial and boundary conditions are:

$$\begin{gathered} t' \le 0 : \quad u = 0\,, \quad v = 0, \quad T' = T'_\infty, \\ C' = C'_\infty \quad for\ all \quad x \ge 0 \quad and \quad r \ge 0 \\ t' > 0 : \quad u = u_0\,, \quad v = 0, \quad T' = T'_w, \quad C' = C'_w \quad at \quad r = r_0 \\ u = 0, \quad v = 0, \quad T' = T'_\infty\,, \quad C' = C'_\infty \quad at \quad x = 0 \quad and \quad r \ge r_0 \\ u \to 0\,, \quad T' \to T'_\infty, \quad C' \to C'_\infty \quad as \quad r \to \infty \end{gathered} \tag{5}$$

where u, v are the velocity components in x, r directions respectively, t'- the time, g- the acceleration due to gravity, β- the volumetric coefficient of thermal expansion, β^*- the volumetric coefficient of expansion with concentration, T'- the temperature of the fluid in the boundary layer, C'- the species concentration in the boundary layer, T'_w - the wall temperature, C'_w- the concentration at the wall, T'_∞ - the free stream temperature of the fluid far away from the plate, C'_∞ - the species concentration in fluid far away from the cylinder, ν-the kinematic viscosity, α- the thermal diffusivity, σ- the electrical conductivity, B_0 - the magnetic induction, ρ- the density of the fluid, c_p- the specific heat at constant pressure, q_r- the radiation heat flux and D- the species diffusion coefficient.

By using the Rosseland approximation (Brewster [21]), the radiative heat flux q_r is given by

$$q_r = -\frac{4\sigma_s}{3k_e}\frac{\partial T'^4}{\partial r} \tag{6}$$

where σ_s is the Stefan-Boltzmann constant and k_e- the mean absorption coefficient. It should be noted that by using the Rosseland approximation, the present analysis is limited to optically thick fluids. If the temperature differences within the flow are sufficiently small, then Equation (6) can be linearized by expanding T'^4 into the Taylor series about T'_∞, which after neglecting higher order terms takes the form

$$T'^4 \cong 4T'^3_\infty\, T' - 3T'^4_\infty \tag{7}$$

In view of Equations (6) and (7), Equation (3) reduces to

$$\frac{\partial T'}{\partial t'} + u\frac{\partial T'}{\partial x} + v\frac{\partial T'}{\partial r} = \frac{\alpha}{r}\frac{\partial}{\partial r}\left(r\frac{\partial T'}{\partial r}\right) + \frac{16\sigma_s T'^3_\infty}{3k_e\rho\, c_p}\frac{1}{r}\frac{\partial}{\partial r}\left(r\frac{\partial T'}{\partial r}\right) \tag{8}$$

Knowing the velocity, temperature and concentration fields, it is interesting to study the local and average skin-frictions, Nusselt numbers and Sherwood numbers, which are defined as follows.

Local and average skin-frictions are given respectively by

$$\tau'_x = -\mu \left(\frac{\partial u}{\partial r}\right)_{r=r_0} \tag{9}$$

$$\overline{\tau}_L = \frac{-1}{L} \int_0^L \mu \left(\frac{\partial u}{\partial r}\right)_{r=r_0} dx \tag{10}$$

Local and average Nusselt numbers are given respectively by

$$Nu_x = \frac{-x \left(\frac{\partial T'}{\partial r}\right)_{r=r_0}}{T'_w - T'_\infty} \tag{11}$$

$$\overline{Nu}_L = -\int_0^L \left[\left(\frac{\partial T'}{\partial r}\right)_{r=r_0} \Big/ (T'_w - T'_\infty)\right] dx \tag{12}$$

Local and average Sherwood numbers are given respectively by

$$Sh_x = \frac{-x \left(\frac{\partial C'}{\partial r}\right)_{r=r_0}}{C'_w - C'_\infty} \tag{13}$$

$$\overline{Sh}_L = -\int_0^L \left[\left(\frac{\partial C'}{\partial r}\right)_{r=r_0} \Big/ (C'_w - C'_\infty)\right] dx \tag{14}$$

In order to write the governing equations and the boundary conditions in dimensionless form, the following non-dimensional quantities are introduced.

$$X = \frac{x\nu}{u_0 r_0^2},\ R = \frac{r}{r_0},\ t = \frac{t'\nu}{r_0^2},\ U = \frac{u}{u_0},\ V = \frac{v r_0}{\nu},\ Gr = \frac{g\beta r_0^2 (T'_w - T'_\infty)}{\nu u_0},$$

$$Gc = \frac{g\,\beta^* r_0^2\,(C'_w - C'_\infty)}{\nu\, u_0}, \quad N = \frac{k_e k}{4\sigma_s T'^3_\infty}, \tag{15}$$

$$M = \frac{\sigma\, B_0^2 r_0^2}{\rho\nu}, \quad T = \frac{T' - T'_\infty}{T'_w - T'_\infty},$$
$$C = \frac{C' - C'_\infty}{C'_w - C'_\infty}, \quad \Pr = \frac{\nu}{\alpha}, \quad Sc = \frac{\nu}{D}$$

In view of the Equation (15), the Equations (1), (2), (8) and (4) reduce to the following non-dimensional form

$$\frac{\partial\,(RU)}{\partial\, X} + \frac{\partial(RV)}{\partial\, R} = 0 \tag{16}$$

$$\frac{\partial\, U}{\partial\, t} + U\,\frac{\partial\, U}{\partial\, X} + V\,\frac{\partial\, U}{\partial\, R} = Gr\, T + Gc\; C + \frac{1}{R}\frac{\partial}{\partial R}\left(R\frac{\partial U}{\partial R}\right) - MU \tag{17}$$

$$\frac{\partial\, T}{\partial\, t} + U\,\frac{\partial\, T}{\partial\, X} + V\,\frac{\partial\, T}{\partial\, R} = \frac{1}{\Pr}\left(1 + \frac{4}{3N}\right)\frac{1}{R}\frac{\partial}{\partial R}\left(R\frac{\partial T}{\partial R}\right) \tag{18}$$

$$\frac{\partial\, C}{\partial\, t} + U\,\frac{\partial\, C}{\partial\, X} + V\frac{\partial\, C}{\partial\, R} = \frac{1}{Sc}\,\frac{1}{\partial R}\left(R\frac{\partial C}{\partial R}\right) \tag{19}$$

The corresponding initial and boundary conditions are

$$t \le 0 : \;\; U = 0\,, \;\; V = 0, \;\; T = 0, \;\; C = 0 \;\; for\; all\; X \ge 0\; and\; R \ge 0$$

$$\begin{gathered} t > 0 \;:\; U = 1\,,\; V = 0\,,\;\; T = 1,\;\; C = 1 \quad at\;\; R = 1 \\ U = 0,\;\; T = 0\,,\; C = 0\; at\;\; X = 0\; and\; R \ge 1 \\ U \to 0,\; T \to 0,\;\; C \to 0\; as\; R \to \infty \end{gathered} \tag{20}$$

where Gr is the thermal Grashof number, Gc- solutal Grashof number, M - the magnetic parameter, Pr - the Prandtl number, N- the radiation parameter and Sc- the Schmidt number.

Local and average skin-frictions in non-dimensional form are given by

$$\tau_X = -\left(\frac{\partial\, U}{\partial\, R}\right)_{R=1} \tag{21}$$

$$\overline{\tau} = -\int_0^1 \left(\frac{\partial\, U}{\partial\, R}\right)_{R=1} dX \tag{22}$$

Local and average Nusselt numbers in non-dimensional form are given by

$$Nu_X = -X\left(\frac{\partial T}{\partial R}\right)_{R=1} \tag{23}$$

$$\overline{Nu} = -\int_0^1 \left(\frac{\partial T}{\partial R}\right)_{R=1} dX \tag{24}$$

Local and average Sherwood numbers in non-dimensional form are given by

$$Sh_X = -X\left(\frac{\partial C}{\partial R}\right)_{R=1} \tag{25}$$

$$\overline{Sh} = -\int_0^1 \left(\frac{\partial C}{\partial R}\right)_{R=1} dX \tag{26}$$

3 Numerical Technique

In order to solve the unsteady, non-linear coupled Equations (16) to (19) under the conditions (20), an implicit finite difference scheme of Crank-Nicolson type has been employed.

$$\frac{\left[U_{i,j}^{n+1} - U_{i-1,j}^{n+1} + U_{i,j}^{n} - U_{i-1,j}^{n} + U_{i,j-1}^{n+1} - U_{i-1,j-1}^{n+1} + U_{i,j-1}^{n} - U_{i-1,j-1}^{n}\right]}{4\Delta X} +$$

$$\frac{\left[V_{i,j}^{n+1} - V_{i,j-1}^{n+1} + V_{i,j}^{n} - V_{i,j-1}^{n}\right]}{2\Delta R} + \frac{V_{i,j}^{n+1}}{1+(j-1)\Delta R} = 0 \tag{27}$$

$$\frac{\left[U_{i,j}^{n+1} - U_{i,j}^{n}\right]}{\Delta t} + U_{i,j}^{n}\frac{\left[U_{i,j}^{n+1} - U_{i-1,j}^{n+1} + U_{i,j}^{n} - U_{i-1,j}^{n}\right]}{2\Delta X} +$$

$$V_{i,j}^{n}\frac{\left[U_{i,j+1}^{n+1} - U_{i,j-1}^{n+1} + U_{i,j+1}^{n} - U_{i,j-1}^{n}\right]}{4\Delta R} = Gr\,\frac{\left[T_{i,j}^{n+1} + T_{i,j}^{n}\right]}{2} +$$

$$Gc\,\frac{\left[C_{i,j}^{n+1} + C_{i,j}^{n}\right]}{2} + \frac{\left[U_{i,j-1}^{n+1} - 2\,U_{i,j}^{n+1} + U_{i,j+1}^{n+1} + U_{i,j+1}^{n+1} - 2U_{i,j}^{n} + U_{i,j+1}^{n}\right]}{2(\Delta R)^2}$$

$$+\frac{\left[U_{i,j+1}^{n+1}-U_{i,j-1}^{n+1}+U_{i,j+1}^{n}-U_{i,j-1}^{n}\right]}{4[1+(j-1)\Delta R]\Delta R}-\frac{M}{2}\left[U_{i,j}^{n+1}+U_{i,j}^{n}\right] \tag{28}$$

$$\frac{[T_{i,j}^{n+1}-T_{i,j}^{n}]}{\Delta t}+U_{i,j}^{n}\frac{\left[T_{i,j}^{n+1}-T_{i-1,j}^{n+1}+T_{i,j}^{n}-T_{i-1,j}^{n}\right]}{2\Delta X}+$$

$$+V_{i,j}^{n}\frac{\left[T_{i,j+1}^{n+1}-T_{i,j-1}^{n+1}+T_{i,j+1}^{n}-T_{i,j-1}^{n}\right]}{4\Delta R}=$$

$$\frac{1}{\mathrm{Pr}}\left(1+\frac{4}{3N}\right)\left(\frac{\left[T_{i,j-1}^{n+1}-2\,T_{i,j}^{n+1}+T_{i,j+1}^{n+1}+T_{i,j-1}^{n}-2T_{i,j}^{n}+T_{i,j+1}^{n}\right]}{2(\Delta R)^{2}}+\right.$$

$$\left.\frac{\left[T_{i,j+1}^{n+1}-T_{i,j-1}^{n+1}+T_{i,j+1}^{n}-T_{i,j-1}^{n}\right]}{4[1+(j-1)\Delta R]\Delta R}\right) \tag{29}$$

$$\frac{[C_{i,j}^{n+1}-C_{i,j}^{n}]}{\Delta t}+U_{i,j}^{n}\frac{\left[C_{i,j}^{n+1}-C_{i-1,j}^{n+1}+C_{i,j}^{n}-C_{i-1,j}^{n}\right]}{2\Delta X}+$$

$$V_{i,j}^{n}\frac{\left[C_{i,j+1}^{n+1}-C_{i,j-1}^{n+1}+C_{i,j+1}^{n}-C_{i,j-1}^{n}\right]}{4\Delta R}\quad=$$

$$\frac{1}{Sc}\frac{\left[C_{i,j-1}^{n+1}-2\,C_{i,j}^{n+1}+C_{i,j+1}^{n+1}+C_{i,j-1}^{n}-2C_{i,j}^{n}+C_{i,j+1}^{n}\right]}{2(\Delta R)^{2}}+$$

$$\frac{\left[C_{i,j+1}^{n+1}-C_{i,j-1}^{n+1}+C_{i,j+1}^{n}-C_{i,j-1}^{n}\right]}{4Sc[1+(j-1)\Delta R]\Delta R} \tag{30}$$

Here, the subscript i- designates the grid point along the X - direction, j - along the R- direction and the superscript n along the t - direction. The appropriate mesh sizes considered for the calculation are $\Delta X = 0.05$, $\Delta R = 0.25$, and time step $\Delta t = 0.01$. During any one-time step, the coefficients $U_{i,j}^{n}$ and $V_{i,j}^{n}$ appearing in the difference equations are treated as constants. The values of U, V, T and C are known at all grid points at $t = 0$ from the initial conditions. The computations of U, V, T and C at time level $(n+1)$ using the known values at previous time level (n) are calculated as follows.

The finite difference Equation (30) at every internal nodal point on a particular i- level constitute a tri-diagonal system of equations. Such a system of equations is solved by Thomas algorithm as described in Carnahan et al. [22]. Thus, the values of C are found at every nodal point on a particular $i$at $(n+1)^{th}$ time level. Similarly, the values of T are calculated

from the Equation (29). Using the values of C and T at $(n+1)^{th}$ time level in the Equation (28), the values of U at $(n+1)^{th}$ time level are found in a similar manner. Thus the values of $C, T$and $U$are known on a particular i- level. The values of V are calculated explicitly using the Equation (27) at every nodal point on a particular i- level at $(n+1)^{th}$ time level. This process is repeated for various i- levels. Thus, the values of C, T, U and $V$are known at all grid points in the rectangular region at $(n+1)^{th}$ time level.

Computations are carried out till the steady state is reached. The steady state solution is assumed to have been reached, when the absolute difference between the values of U as well as temperature T and concentration C at two consecutive time steps are less than 10^{-5} at all grid points. The derivatives involved in the Equations (21) to (26) are evaluated using five-point approximation formula and the integrals are evaluated using Newton-Cotes closed integration formula. The truncation error in the finite-difference approximation is $O\left(\Delta t^2 + \Delta R^2 + \Delta X\right)$ and it tends to zero as ΔX, ΔR, $\Delta t \to 0$. Hence the scheme is compatible. The finite-difference scheme is unconditionally stable as explained by Ganesan and Rani [8]. Stability and compatibility ensures convergence.The derivatives involved in the Equations (21) - (26) are evaluated using five-point approximation formula and the integrals are evaluated using Newton-Cotes closed integration formula.

4 Results and Discussion

In order to get a physical insight into the problem, a representative set of numerical results is shown graphically in Figs. 1-11, to illustrate the influence of governing parameters viz., radiation parameter N, thermal Grashof number Gr, solutal Grashof number Gc, magnetic field parameter M and Schmidt number Sc on the velocity, temperature and concentration. The value of the Prandtl number Pr is choosen to be 0.71, which corresponds air and the values of Sc are chosen such that they represent water vapor (0.6) and carbon dioxide (0.94).

In order to ascertain the accuracy of the numerical results, the present study is compared with the previous study. The concentration profiles for $Gr = 5.0$, $Gc = 5.0$, $N = 0.0$, $M = 0.0$, $Pr = 0.7$ are compared with the

available solution of Ganesan and Loganathan [7] in Fig.1. It is observed that the present results are in good agreement with that of Ganesan and Loganathan [7].

The transient velocity profiles for different values of Gr, Gc, M, N and Sc at a particular time t= 0.75 are shown in Fig.2. The thermal Grashof number signifies the relative effect of the thermal buoyancy (due to density differences) force to the viscous hydrodynamic force in the boundary layer flow. The positive values of Gr correspond to cooling of the cylinder by natural convection. Heat is therefore conducted away from the vertical cylinder into the fluid which increases temperature and thereby enhances the buoyancy force. It is observed that the transient velocity accelerates due to enhancement in the thermal buoyancy force. The solutal Grashof number Gc defines the ratio of the species buoyancy force to the viscous hydrodynamic force. It is noticed that the transient velocity increases considerably with a rise in the species buoyancy force. In both the cases it is interesting to note that as Gr or Gc increases, there is rapid rise in the velocity near the surface of vertical cylinder and then descends smoothly to the free stream velocity. As expected, the transient velocity decreases with an increase in the magnetic parameter M. It is because that the application of transverse magnetic field will result a resistive type force (Lorentz force) similar to drag force which tends to resist the fluid flow and thus reducing its velocity. Also, the boundary layer thickness decreases with an increase in the magnetic parameter. The radiation parameter N(i.e., Stark number) defines the relative contribution of conduction heat transfer to thermal radiation transfer. It can be seen that an in increase in N leads to a decrease in the velocity. The Schmidt number Sc embodies the ratio of the momentum diffusivity to the mass (species) diffusivity. It physically relates the relative thickness of the hydrodynamic boundary layer and mass-transfer (concentration) boundary layer. It is observed that as the Schmidt number increases the transient velocity decreases.

In Fig.3, the transient and steady state velocity profiles are presented for different values Gr, Gc, M, N and Sc. The steady state velocity increases with an increase in Gr or Gc. It can be seen that an increase in the thermal or species buoyancy force, reduces the time required to reach the steady state. The steady state velocity decreases with an increase in Mor N or Sc. The time taken to reach the steady state velocity increases

as M or N increases.

The transient and steady state temperature profiles are presented for different values M, N and Sc in Fig.4. It is observed that, as N decreases from 5.0 to 2.0, the temperature increases markedly throughout the length of the cylinder. As a result the thermal boundary layer thickness is decreasing due to a rise in N values. It is noticed that the temperature decreases with an increase in M while it increases with an increase in Sc. The time required to reach the steady state temperature increases with an increase in Mor N and it decreases with an increase in Sc.

In Fig.5, the transient and steady state concentration profiles are presented for different values of M, N and Sc. It is found that the concentration decreases as the radiation parameter N or the Schmidt number Sc increases, while it increases with an increase in M. The time required to reach the steady state concentration increases with an increase in M or N and it decreases with an increase in Sc.

Steady-state local skin-friction (τ_x) values against the axial coordinate X are plotted in Fig.6. The local shear stress τ_x increases with an increase in Sc, while it decreases with an increase in Gr or Gc or M. The average skin-friction ($\bar{\tau}$) values are shown in Fig. 7. It is found that the average skin-friction increases with an increase in Sc, while it decreases with an increase in Gr or Gc or M, throughout the transient period. It is also observed that the average skin-friction increases as the radiation interaction parameter N increases. The local Nusselt number (Nu_X) is shown in Fig.8. The local heat transfer rate decreases with an increase in Sc, while it increases with an increase in Gr or Gc or M. Also it is found that as the radiation parameter N increases, the local Nusselt number increases. The average Nusselt number ($\overline{Nu}$) values are shown in Fig.9. It is observed that the average Nusselt number increases with an increase in Gr or Gc or$N$. The local Sherwood number Sh_X is plotted in Fig.10. It is noticed that Sh_X increases with an increase in Sc, where as it decreases with an increase in Gr or Gc or N. The average Sherwood number ($\overline{Sh}$) values are shown in Fig.11. It can be seen that the average Sherwood number increases with an increase in Gr or Gc or Sc, while it decreases with an increase in M.

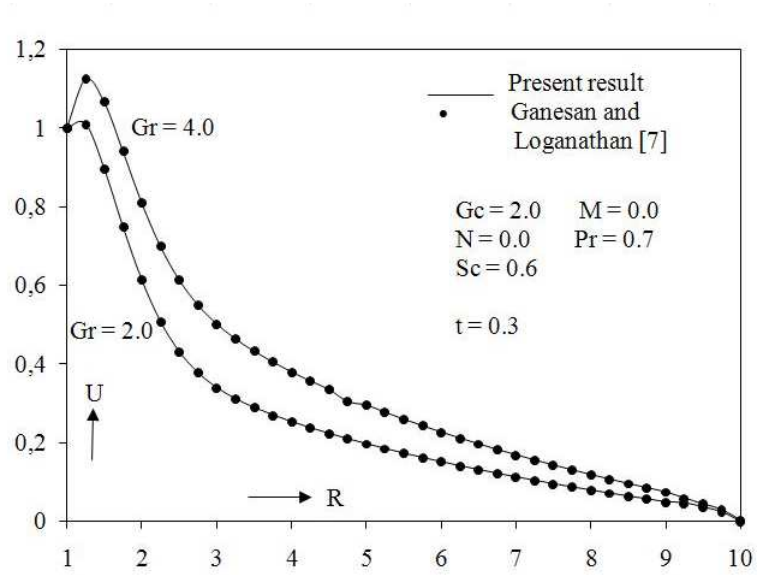

Figure 1: Comparison of velocity profiles

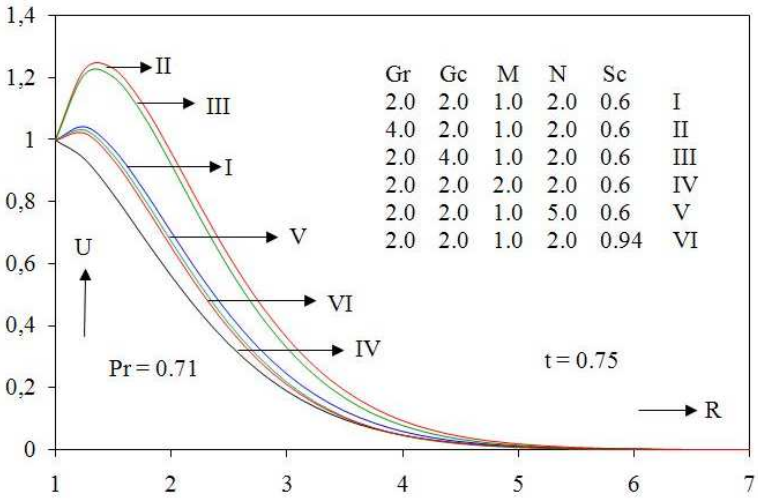

Figure 2: Transient velocity profiles at X=1.0 for different Gr, Gc, M, N and Sc

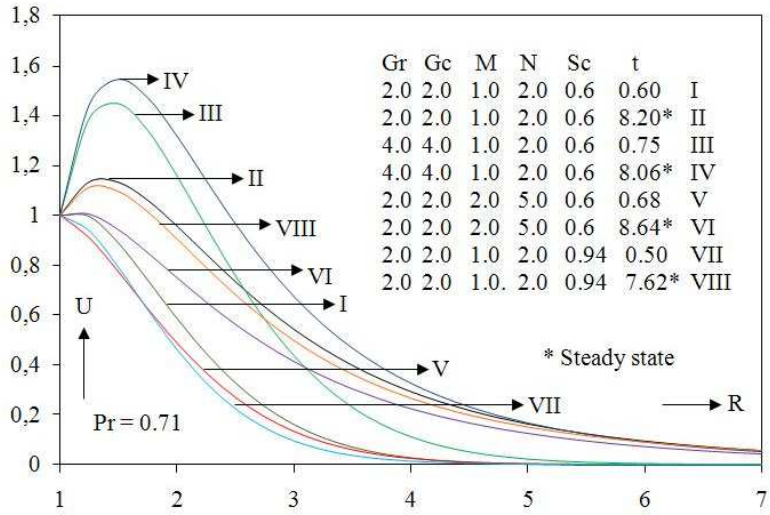

Figure 3: Velocity profiles at X=1.0 for different Gr, Gc, M , N and Sc

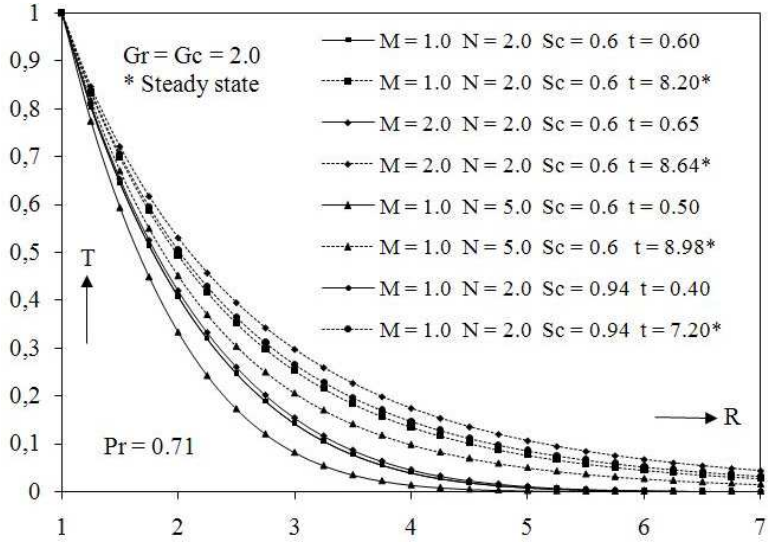

Figure 4: Temperature profiles at X=1.0 for different M, N and Sc

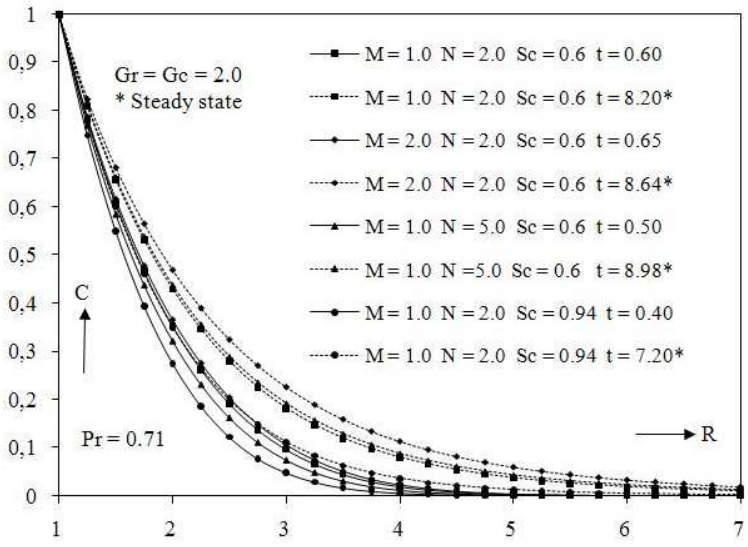

Figure 5: Concentration profiles at X=1.0 for different M, N and Sc

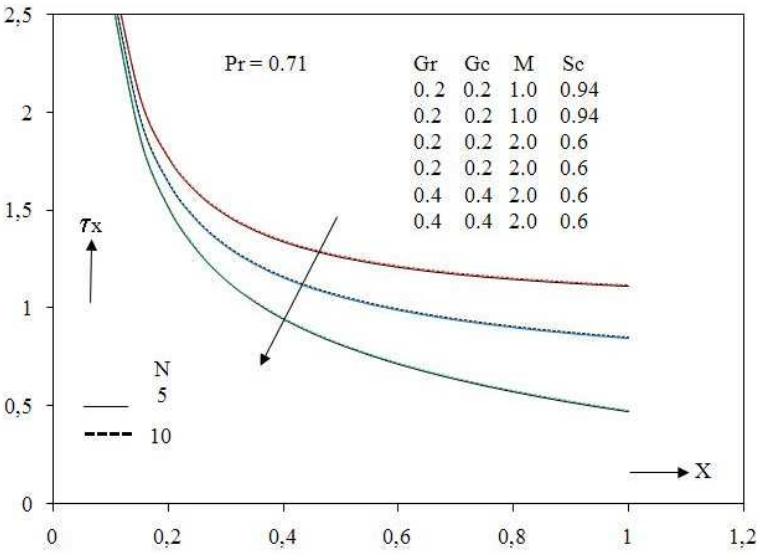

Figure 6: Local skin-friction

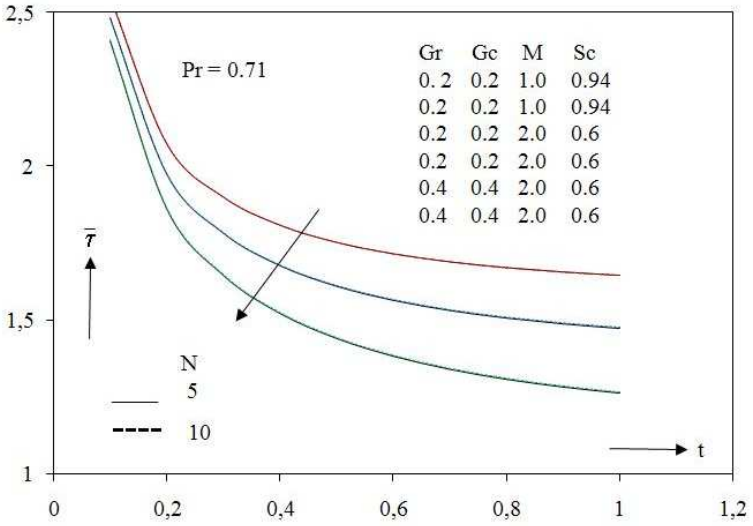

Figure 7: Average skin-friction

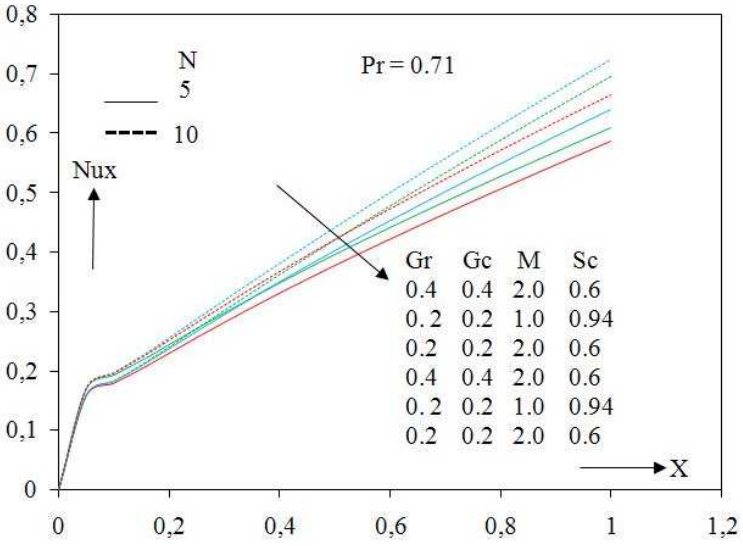

Figure 8: Local Nusselt number

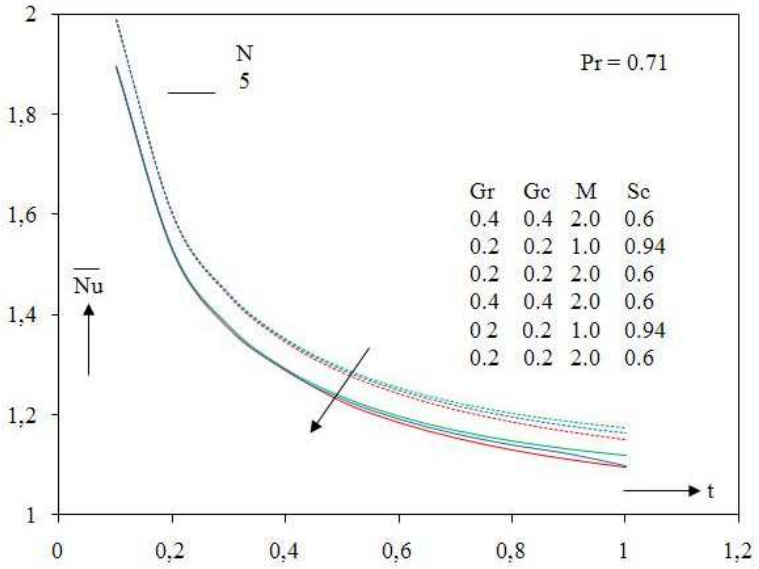

Figure 9: Average Nusselt number

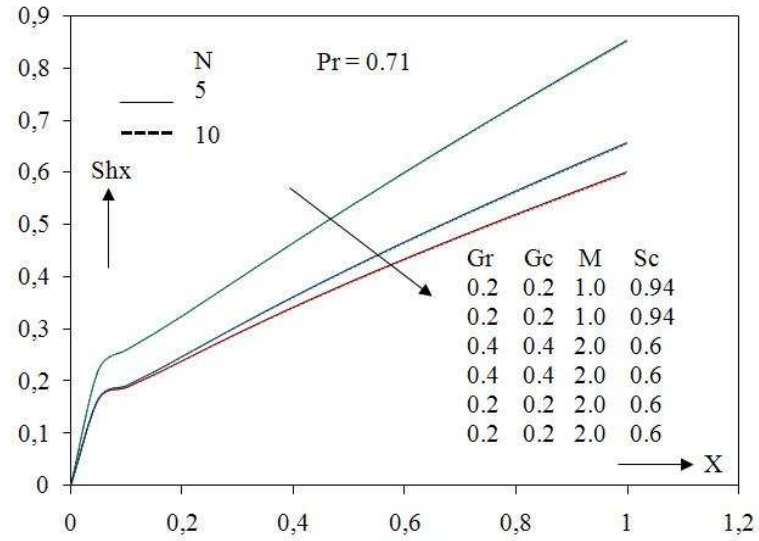

Figure 10: Local Sherwood number

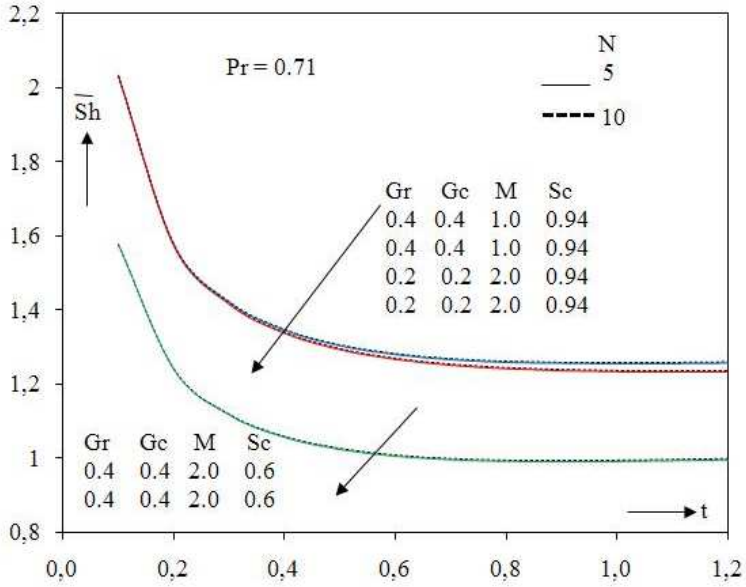

Figure 11: Average Sherwood number

5 Conclusions

A numerical study has been carried out to study the interaction of radiation and mass transfer effects on MHD flow of an incompressible viscous fluid past a moving vertical cylinder. The fluid is gray, absorbing-emitting but non-scattering medium and the Rosseland approximation is used to describe the radiative heat flux in the energy equation. A family of governing partial differential equations is solved by an implicit finite difference scheme of Crank-Nicolson type, which is stable and convergent. The results are obtained for different values of radiation parameter N, thermal Grashof number Gr, solutal Grashof number Gc, magnetic field parameter M, and Schmidt number Sc. The conclusions of this study are as follows

1. The transient velocity increases with the increase in Gr or Gc.

2. The transient velocity decreases with an increase in the magnetic parameter M.

3. The time required for velocity to reach the steady-state increases as radiation parameter N increases.

4. As small values of the radiation parameter N, the velocity and temperature of fluid increases sharply near the cylinder as the time t increases, which is totally absent in the absence of radiation effects.

5. The skin-friction decreases with an increase M and increases with the increasing value of radiation parameter N and Schmidt number Sc.

References

[1] Evan L.B., Reid R.C. and Drake E.M. (1968), Transient natural convection in a vertical cylinder, A.I.Ch.E. J., Vol.14, pp.251-261.

[2] Velusamy K. and Garg V.K. (1992), Transient natural convection over a heat generating vertical cylinder, Int. J. Heat Mass Transfer, Vol.35, pp.1293-1306.

[3] Michiyoshi I., Takahashi I. and Seizawa A. (1976), Natural convection heat transfer form a horizontal cylinder to mercury under a magnetic field, Int. J. Heat Mass Transfer, Vol.19, pp.1021-1029.

[4] Ganesan P. and Loganathan P. (2003), Magnetic field effect on a moving vertical cylinder with constant heat flux, Heat Mass Transfer, Vol.39, pp.381-386.

[5] Chen T.S. and Yuh C.F. (1980), Combined heat and mass transfer in natural convection along a vertical cylinder, Int. J. Heat Mass transfer, Vol.23, pp.451-461.

[6] Takhar H.S., Chamkha A.J. and Nath G. (2000), Combined heat and mass transfer along a vertical cylinder with free stream, Heat Mass Transfer, Vol.36, pp.237-246.

[7] Ganesan P. and Loganathan P. (2001), Unsteady free convection flow over a moving vertical cylinder with heat and mass transfer, Heat Mass Transfer, Vol.37(1), pp.59-65.

[8] Ganesan P. and Rani H.P. (1998), Transient natural convection cylinder with heat and mass transfer, Heat Mass Transfer, Vol.33, pp.449-455.

[9] Shanker B. and Kishan N. (1997), The effects of mass transfer on the MHD flow past an impulsively started infinite vertical plate with variable temperature or constant heat flux, J. Engg. Heat Mass Transfer, Vol.19, pp.273-278.

[10] Ganesan P. and Rani H.P. (2000), Unsteady free convection MHD flow past a vertical cylinder with heat and mass transfer, Int. J. Therm. Sci., Vol.39,pp.265-272.

[11] Arpaci V.S. (1968), Effects of thermal radiation on the laminar free convection from a heated vertical plate, Int. J. Heat Mass Transfer, Vol.11, pp.871-881.

[12] Cess R.D. (1966), Interaction of thermal radiation with free convection heat transfer, Int. J. Heat Mass transfer, Vol.9, pp.1269-1277.

[13] Cheng E.H and Ozisik M.N. (1972), Radiation with free convection in an absorbing emitting and scattering medium, Int. J. Heat Mass Transfer, Vol.15, pp.1243-1252.

[14] Raptis A. (1998), Radiation and free convection flow through a porous medium, Int.Comm. Heat Mass Transfer, Vol.25(2), pp.289-295.

[15] Hossain M.A. and Takhar H.S. (1996), Radiation effects on mixed convection along a vertical plate with uniform surface temperature, Heat Mass Transfer, Vol.31, pp.243-248.

[16] Hossain M.A. and Takhar H.S. (1999), Thermal radiation effects on the natural convection flow over an isothermal horizontal plate, Heat Mass Transfer, Vol.35, pp.321-326.

[17] Das U.N., Deka R. and Soundalgekar V.M. (1996), Radiation effects on flow past an impulsively started vertical plate-an exact solutions, J. Theo. Appl. Fluid Mech., Vol.1(2), pp.111-115.

[18] Ramachandra Prasad V., Bhaskar Reddy N. and Muthucumaraswamy R. (2007), Radiation and mass transfer effects on two-dimensional flow past an impulsively started isothermal vertical plate,Int.J. Thermal Sciences, Vol.46(12), pp.1251-1258.

[19] Yih K.A. (1999), Radiation effects on natural convection over a vertical cylinder embedded in porous media, Int. Comm. Heat Mass Transfer, Vol.26(2), pp.259-267.

[20] Ganesan P. and Loganathan P. (2002), Radiation and mass transfer effects on flow of an incompressible viscous fluid past a moving vertical cylinder, Int. J. Heat Mass Transfer,Vol.45, pp.4281-4288.

[21] Brewster M.Q. (1992), Thermal radiative transfer and properties, John Wiley & Sons, New York.

[22] Carnahan B., Luther H.A. and Wilkes J.O. (1969), Applied Numerical Methods, John Wiley & Sons, New York.

Submitted on December 2007, revised on February 2009

Radijacija i prenos mase pri nestacionarnoj MHD konvekciji nestišljivog viskoznog fluida po pokretnom vertikalnom cilindru

Analizira se interakcija slobodne konvekcije sa termičkim zračenjem pri viskoznom nestišljivom nestacionarnom MHD strujanju preko pokretnog vertikalnog cilindra sa toplotnim i masenim prenosom. Fluid je siva, apsorbujuće-emitujuća nerasejavajuća sredina te se Rosseland-ova aproksimacija koristi za opis zračećeg toplotnog protoka u jednačini energije. Jednačine problema se rešavaju šemom konačnih razlika Krenk-Nikolsonovog tipa. Numerički rezultati za prelaznu brzinu, temperaturu, koncentraciju, lokalno i prosečno trenje na zidu, brzinu promene toplote i prenos mase su prikazani za rezličite parametre kao: termički Grashofov broj, maseni Grashofov broj, magnetski parametar, parametar zračenja i Šmitov broj. Primećuje se da kada parametar zračenja raste tada brzina i temperatura u graničnom sloju opadaju. Takodje, nadjeno je da porast magnetskog polja vodi opadanju polja brzine i rastu debljine termičke granice.

doi:10.2298/TAM0903239G Math.Subj.Class.: 76W05